

Trivelpiece–Gould modes and low-frequency electron–ion instability of non-neutral plasma

Yuriy N. Yeliseyev  

National Science Center ‘Kharkiv Institute of Physics and Technology’, Institute of Plasma Physics, Akademichna st. 1, Kharkiv, 61108, Ukraine

(Received 16 May 2023; revised 28 November 2023; accepted 29 November 2023)

The frequency spectra of the Trivelpiece–Gould modes of a waveguide partially filled with non-neutral plasma are determined numerically by solving the dispersion equation. The modes having azimuthal number $m = 1$ are considered. The results are presented for the entire acceptable range of electron densities, magnetic field strengths, for different values of the charge neutralization coefficient. The Cherenkov resonance condition of an ion with a diocotron mode having a finite value of the longitudinal wave vector was studied. The characteristics of resonant low-frequency electron–ion instability caused by relative azimuth motion of electrons and ions in crossed fields and by the anisotropy of the distribution function of ions are discussed. Ions are created by ionization of residual gas in the plasma volume. Due to the anisotropy, instability occurs not only in the vicinity of the resonance, but also outside it. For typical values of plasma parameters in experiments, estimations of the frequency growth rate are given. A conclusion is drawn that this instability can be the cause of the low-frequency oscillations observed in linear devices with non-neutral plasma produced in an electron beam channel.

Key words: non-neutral plasma, low-frequency instability, plasma instabilities, plasma waves

1. Introduction

The Trivelpiece–Gould (TG) modes – the electron eigenmodes of a cylindrical waveguide completely or partially filled with a homogeneous cold neutral plasma in a magnetic field – are well known (Trivelpiece & Gould 1959). The behaviour of the frequencies of the TG modes of a plasma, which is at rest or moving along a magnetic field, is determined and analysed. The motion of plasma electrons leads to a radical rearrangement of the frequency spectrum of TG modes ω observed in the laboratory frame of reference. Usually, electron modes are of high frequency both in the laboratory and in the moving frames. However, the modes that propagate in the direction opposite to the movement of electrons can become low frequency in the laboratory frame due to the Doppler shift. Their frequencies ω can be of the order of characteristic ion frequencies. If the electrons and ions of the plasma move at different velocities, an electron–ion instability is possible due to the relative motion of the electrons and ions (the Buneman instability).

† Email address for correspondence: yeliseyev@kipt.kharkov.ua

The TG modes are also known in non-neutral plasma (Davidson 1974), which, along with a longitudinal magnetic field, has a radial electric field E_r due to an excess of electrons. Under the action of crossed fields, charged particles rotate along the azimuth. Modes propagating in the plasma in the direction opposite to the rotation of electrons can become low frequency in the laboratory frame due to the Doppler shift. Their frequencies can become of the order of characteristic ion frequencies. Electrons rotate faster than ions. This is a general property of a non-neutral plasma. Electron–ion instability is possible under these conditions. It must be universal in non-neutral plasma and must develop at frequencies of the order of characteristic ion frequencies.

Low-frequency oscillations ($\omega \sim \omega_{ci}$) are often observed for a wide range of plasma parameter variations in non-neutral plasma devices, for example, in cylindrical Penning–Malmberg traps (Peurrung, Notte & Fajans 1993; Kabantsev & Driscoll 2003; Bettega *et al.* 2005) and in linear devices in which non-neutral plasma is created as a secondary plasma in an electron beam channel (Vlasov, Dobrokhotov & Zharinov 1966; Nezlin 1982; Pierre, Leclert & Braun 1987; Sakawa & Joshi 2000; Jaeger 2010; Annaratone *et al.* 2011; David 2017). In Penning–Malmberg traps, the nature of low-frequency oscillations has been reliably established and related to the instability of the diocotron mode due to a small addition of positive ions to electron plasma (ion-induced instability). At the same time, the nature of low-frequency oscillations in linear devices remains as not reliably known (Jaeger 2010; Annaratone *et al.* 2011; David 2017). Various instabilities were suggested to understand the cause of these oscillations (see Jaeger (2010) and David (2017) for reviews).

This article discusses the instability of the relative azimuth motion of electrons and ions in the model of an infinite waveguide partially filled with non-neutral plasma.

This instability was studied in the well-known paper by Levy, Daugherty & Buneman (1969). The hydrodynamic description was used for electrons and ions. The longitudinal wave vector k_z was chosen equal to zero ($k_z = 0$). It has been shown that if the addition of ions is small, then the electron–ion instability occurs only in the vicinity of the resonance of the diocotron mode with the ion rotation.

We discuss this instability in the case $k_z \neq 0$ and take into account the kinetics of ions that are produced in crossed fields by electron impact of atoms (molecules) of residual gas. The distribution function of such ions is anisotropic and has a non-Maxwellian dependence on transverse energies (Dem'yanov *et al.* 1988). These two circumstances (ion anisotropy and $k_z \neq 0$) bring the plasma model closer to reality. As a result, the obtained instability picture is closer to that observed in experiments: the electron–ion instability exists not only near the resonance of electron mode with ion rotation, but also in a wide area outside the resonance.

In the present paper, the well-known dispersion equation (Davidson 1974) for electron eigenmodes of potential oscillations in an infinite waveguide partially filled with cold uniform non-neutral plasma is solved numerically (§ 3). The frequency spectra of TG modes ω having an azimuthal number $m = 1$ are determined for finite value of the longitudinal wave vector $k_z \neq 0$ and for different values of the charge neutralization coefficient f . Particular attention is paid to the behaviour of modes in the area of low (ion) frequencies. The Cherenkov resonance condition of an ion with a diocotron mode having a finite value of the longitudinal wave vector $k_z \neq 0$ is studied (§ 5.1). Numerical estimations of resonance frequencies for typical values of parameters of experiments are given (§ 5.2). The frequency, growth rate and peculiarities of the expected low-frequency electron–ion instability are estimated (§ 5.3). In Appendix A the areas are defined, where TG modes are bulk in plasma, and where they are surface modes. In Appendix B the behaviour of TG

modes of neutral plasma is analysed and compared with the results obtained by Trivelpiece & Gould (1959).

In theoretical papers, the frequencies of the TG modes are usually represented as being dependent on the longitudinal wave vector, $\omega(k_z)$ (Trivelpiece & Gould 1959; Davidson 1974). However, in experiments, the frequencies of eigen plasma oscillations are measured and performed depending on external fields, plasma density, etc. Just these parameters are controlled and varied in experiments. At the same time, the wave vector k_z remains most often invariable, and frequently indefinite.

In the theory of non-neutral plasma (Levy *et al.* 1969; Davidson 1974), the parameter

$$q \equiv 2\omega_{pe}^2/\omega_{ce}^2 \tag{1.1}$$

is introduced. It determines the characteristic frequencies of both electrons and ions. Ultimately, it determines the equilibrium and stability of a non-neutral plasma. Only in the range

$$0 < q < q_{max} \equiv 1/(1 - f) \tag{1.2}$$

the motion of electrons along the radius is finite and the equilibrium state of the ensemble of electrons is possible, and, hence, of the plasma in total. In this paper, all results are represented as dependences on the variable q (1.1). The calculations are carried out within the entire acceptable range of values of q (1.2).

2. Dispersion equation under study

We solve the dispersion equation for the potential electron modes of an infinite waveguide partially filled with a homogeneous rigidly rotating non-neutral plasma (Davidson 1974):

$$k_z R_p \frac{K_m(k_z R_w) I'_m(k_z R_p) - K'_m(k_z R_p) I_m(k_z R_w)}{K_m(k_z R_w) I_m(k_z R_p) - K_m(k_z R_p) I_m(k_z R_w)} = \varepsilon_1 T k_z R_p \frac{J'_m(T k_z R_p)}{J_m(T k_z R_p)} + m \varepsilon_2. \tag{2.1}$$

In (2.1) J_m is the Bessel function of the first kind of order m , I_m and K_m are the modified Bessel functions, J'_m, I'_m, K'_m are their derivatives with respect to the entire argument, R_p, R_w are the plasma and waveguide radii, $R_p \leq R_w$, and

$$T^2 \equiv -\varepsilon_3/\varepsilon_1. \tag{2.2}$$

This definition of T^2 (2.2) differs from the definition given by Trivelpiece & Gould (1959) and Davidson (1974) by a factor k_z^2 . The permittivity tensor of cold electron plasma has the form

$$\varepsilon_{ij} = \begin{pmatrix} \varepsilon_1 & i\varepsilon_2 & 0 \\ -i\varepsilon_2 & \varepsilon_1 & 0 \\ 0 & 0 & \varepsilon_3 \end{pmatrix}, \quad \varepsilon_1 = 1 - \frac{\omega_{pe}^2}{v^2}, \quad \varepsilon_2 = \frac{\omega_{pe}^2 \Omega_e}{v^2 \omega'}, \quad \varepsilon_3 = 1 - \frac{\omega_{pe}^2}{\omega'^2}. \tag{2.3}$$

Here $\omega_{pe}^2 = 4\pi e^2 n_e/m_e$ is the square of the Langmuir electron frequency, $v^2 \equiv \omega^2 - \Omega_e^2$, $\Omega_e = \text{sgn}(e)|\omega_{ce}|(1 - 4eE_r/(\omega_{ce}^2 m_e r))^{1/2}$ is the ‘modified’ cyclotron frequency of an electron in crossed fields, the radial electric field E_r is due to the uncompensated plasma space charge, $E_r = (m_e/2e)\omega_{pe}^2 r(1 - f) < 0, f = n_i/n_e$, are the electron and ion densities, $0 \leq f \leq 1$, $\omega' = \omega - m\omega_{rot}^e$ is the mode frequency in the frame rotating with electrons, $\omega_{rot}^e = (-\omega_{ce} + \Omega_e)/2 > 0$ is the ‘slow’ rotation frequency of electrons, r is the distance to the waveguide axis, $\omega_{ce} = eB/(m_e c) < 0$ is the electron cyclotron frequency and e and

m_e are the charge and mass of an electron ($e < 0$). When the waveguide is uniformly filled with electrons and ions, the combination E_r/r , frequency Ω_e and other frequencies in (2.1) are independent of the radius r inside the plasma. Ions are taken into account only as a neutralizing background (in f).

We consider q as an independent variable and represent the results of calculations as being dependent on it. We normalize all frequencies up to $|\omega_{ce}|$ and express all quantities included in the dispersion equation (2.1) as functions of q :

$$\Omega_e/|\omega_{ce}| = \text{sgn}(e)[1 - q(1 - f)]^{1/2} < 0, \tag{2.4}$$

$$\omega_{\text{rot}}^e/|\omega_{ce}| = (1/2)\text{sgn}(e)\{-1 + [1 - q(1 - f)]^{1/2}\}, \tag{2.5}$$

$$x' \equiv \omega'/|\omega_{ce}|, \tag{2.6}$$

$$x \equiv \omega/|\omega_{ce}| = x' + m\omega_{\text{rot}}^e/|\omega_{ce}|. \tag{2.7}$$

The dependences of the permittivity tensor components (2.3) on q take the form

$$\varepsilon_1 = 1 - \frac{q/2}{x'^2 - 1 + q(1 - f)}, \quad \varepsilon_2 = \frac{\text{sgn}(e)q/2}{x'^2 - 1 + q(1 - f)} \frac{[1 - q(1 - f)]^{1/2}}{x'}, \quad \varepsilon_3 = 1 - \frac{q/2}{x'^2}. \tag{2.8a-c}$$

The parameters of the considered problem are: $m, f, k_z R_p, R_p/R_w$. For unambiguity, we consider the azimuthal number m to be positive ($m > 0$). Frequencies x', x can be positive or negative.

The calculations presented in this paper were carried out for the following numerical values of parameters: $m = +1, k_z R_p = 1, R_p/R_w = 1/2$. The calculations were carried out for different values of the charge neutralization coefficient: $f = 0; 0.25; 0.5; 0.75; 1$.

3. Trivelpiece–Gould modes of waveguide partially filled with non-neutral plasma

3.1. Solutions of (2.1) are presented in figure 1(a–d). The solutions form four families: fast (FLH) and slow (SLH) lower hybrid modes; fast (FUH) and slow (SUH) upper hybrid modes. Their frequencies are located in the following frequency ranges (Davidson 1974):

$$\left. \begin{aligned} &\text{modes of families SLH and FLH are in the interval: } \omega'^2 < \min(\omega_{pe}^2, \Omega_e^2), \\ &\text{modes of families SUH and FUH are in the interval: } \max(\omega_{pe}^2, \Omega_e^2) < \omega'^2 < (\omega_{UH}^{\text{NNP}})^2. \end{aligned} \right\} \tag{3.1}$$

The term $\omega_{UH}^{\text{NNP}} = \sqrt{\omega_{pe}^2 + \Omega_e^2}$ defines the hybrid frequency of non-neutral plasma.

There are also two modes located separately from these families. They are indicated in the figures by the numbers ‘1’ and ‘2’.

3.2. The families of SUH and FUH modes are located very close to each other and to the hybrid frequency with a Doppler shift $m\omega_{\text{rot}}^e - \omega_{UH}^{\text{NNP}}$ (Dubin 2016) and remain in its close vicinity when the degree of filling of the waveguide with plasma $(R_p/R_w)^2$ and the parameter $k_z R_p$ vary. In the scale of figure 1 the modes of the SUH family merge with frequency $m\omega_{\text{rot}}^e - \omega_{UH}^{\text{NNP}}$. Similarly the modes of the FUH family merge with frequency $m\omega_{\text{rot}}^e + \omega_{UH}^{\text{NNP}}$.

As is clearly seen from figure 1, the frequencies of the families of SUH modes with the azimuthal number $m = 1$ do not cross the area of low frequencies at any values of the charge neutralization coefficient $0 \leq f \leq 1$. And so it was when the waveguide was completely filled with plasma (Yeliseyev 2010). SUH mode frequencies are closest to zero at $q = q_{\text{max}}$ and $f = 0$ (see figure 1a). They are equal here, $\omega/|\omega_{ce}| = (1 - 2^{1/2})/$

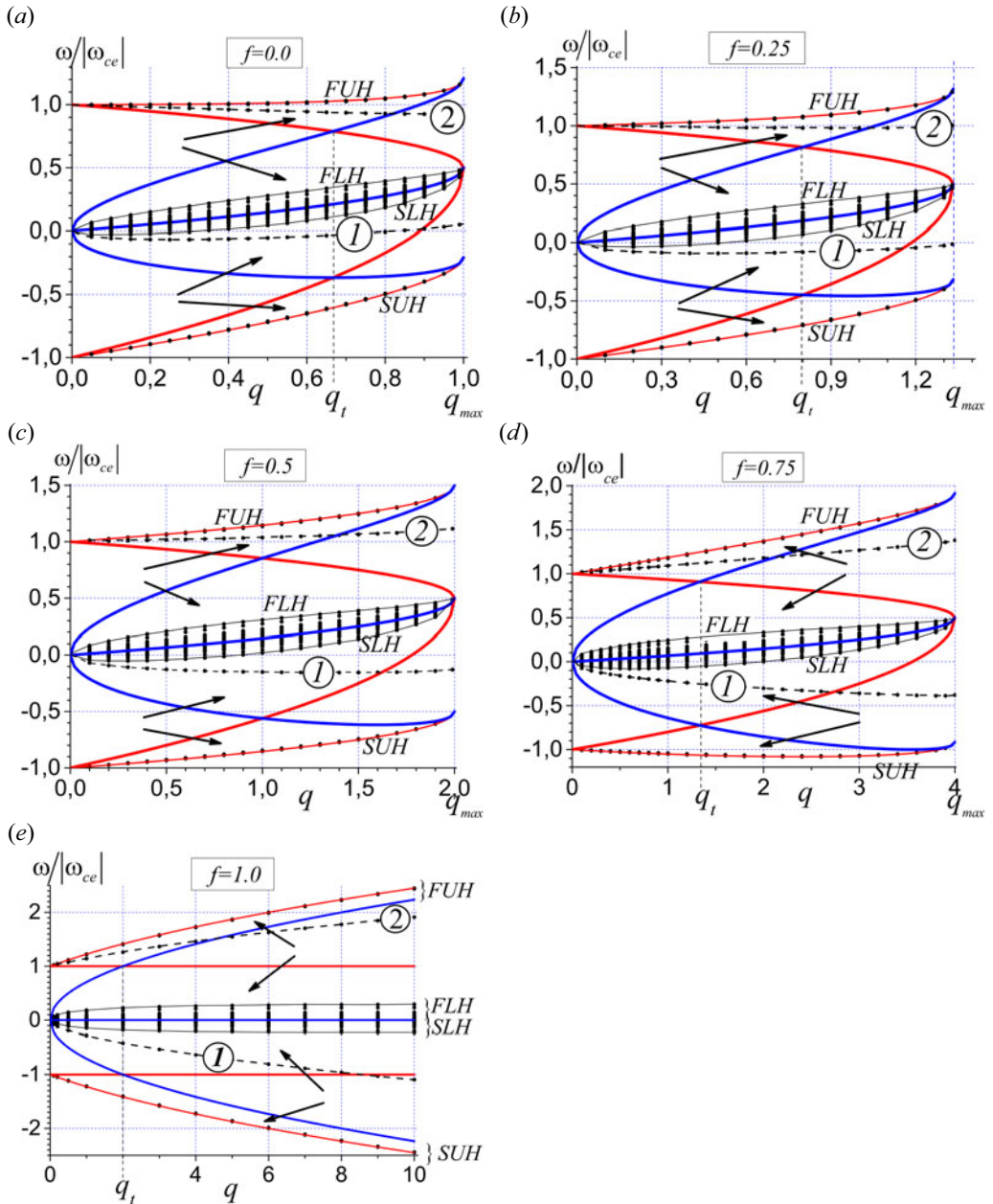


FIGURE 1. Frequencies of TG modes in the laboratory frame of reference $\omega/|\omega_{ce}|$ at different values of charge neutralization coefficient f : (a) $f = 0$; (b) $f = 0.25$; (c) $f = 0.5$; (d) $f = 0.75$; (e) $f = 1$ (neutral plasma). The values of other calculation parameters are: $m = 1$; $k_z R_p = 1.0$; $R_w/R_p = 2$. Solid red and blue lines indicate the boundaries of the areas of existence of bulk (indicated by arrows) and surface eigenmodes (see Appendix A). Thin solid black lines show the lowest radial modes of the SLH and FLH families. The points are the results of the numerical calculation. The quantities q_{max} and q_t are defined in (1.2) and (A 1).

$2 \approx -0.2$. The frequencies of the FUH modes for these q and f are equal, $\omega/|\omega_{ce}| = (1 + 2^{1/2})/2 \approx 1.2$. When f increases, the frequencies of SUH modes move away from zero towards negative frequencies.

3.3. The families of SLH and FLH modes are located in the vicinity of frequency $\omega = m\omega_{rot}^e$. In [figure 1](#), this frequency is shown by a blue solid line dividing the SLH and FLH families. The different radial modes are not so closely spaced as the upper hybrid modes. As the parameter $k_z R_p$ decreases, the mode frequencies approach frequency $m\omega_{rot}^e$ ($\omega \rightarrow m\omega_{rot}^e$ when $k_z R_p \rightarrow 0$). The frequencies of SLH and FLH modes are weakly dependent on the degree of filling of the waveguide with plasma (R_p^2/R_w^2) (at a fixed value of $k_z R_p$). Factor $R_p^2/R_w^2 < 1$ leads to a shift of SLH and FLH modes with respect to frequency $m\omega_{rot}^e$ towards positive frequencies. This is a demonstration of plasma magnetoactivity.

Every radial mode of the SLH family passes through the low (ion)-frequency area and reaches zero frequency when $q \neq 0$ ([figure 1a–d](#)), just as was the case when the waveguide was completely filled with plasma (Yeliseyev 2010). The FLH modes do not reach zero frequency when $q \neq 0$, but pass through the low-frequency area at small q .

3.4. Mode ‘1’ in [figure 1](#) is a diocotron mode with a finite value of the longitudinal wave vector k_z . Mode ‘2’ is called the cyclotron mode. Modes are located near, but separately from, the families of SLH and FUH modes, and depend in noticeably different ways on parameter q . When $q \rightarrow 0$ they approach and merge with the corresponding family, demonstrating relationships with the families of SLH and FUH modes.

In the long-wavelength approximation ($k_z = 0$) the dispersion equation and its solutions corresponding to modes ‘1’ and ‘2’ are given by expressions (2.9.7) and (2.9.8) in Davidson (1974). For small but finite values of k_z , mode ‘1’ was studied by Prasad & O’Neil (1983) in the rarefied plasma approximation ($q \ll 1$) and $f = 0$. In [figure 1\(a–e\)](#) the results of calculations are shown for a considerable value of k_z ($k_z R_p = 1$) and for different values of charge neutralization coefficient f .

As can be seen from [figure 1](#), with parameter f increasing from 0 to 1 the diocotron mode (‘1’) shifts towards negative frequencies. The frequency of the diocotron mode crosses zero when $f < 0.25$ (i.e. when $f < R_p^2/R_w^2$). Its frequency ω_1 is negative within the entire acceptable range of variation of q when $f > 0.25$. Such a behaviour of the mode also follows from the analytical expression (3.2).

With increasing degree of filling of the waveguide for non-neutral plasma ($R_p^2/R_w^2 \rightarrow 1$), the diocotron mode approaches the family of SLH modes and merges with it, becoming its lowest radial mode (Prasad & O’Neil 1983).

The diocotron mode shifts upward towards the SLH family when the parameter $k_z R_p$ is decreased from 1 (and $R_p^2/R_w^2 = \text{const.}$). When $k_z R_p \rightarrow 0$ the frequencies of SLH modes tend to the value ω_{rot}^e . The frequency of the diocotron mode ω_1 tends to the well-known value $\omega_d = (R_p/R_w)^2 \omega_{rot}^e$ (Levy *et al.* 1969; Davidson 1974), that is, positive and less than ω_{rot}^e .

Note that for $k_z R_p = 1$, the frequency of the diocotron mode ω_1 is negative in most of the range of q and f (see [figure 1a–d](#)). The reversal of the sign of the diocotron mode frequency with increasing $k_z R_p$ was discovered by Prasad & O’Neil (1983).

The behaviour of the TG modes of a waveguide partially filled with neutral plasma ($f = 1$) is shown in [figure 1\(e\)](#). The behaviour is analysed in [Appendix B](#).

3.5. It can be shown that the analytical expression for the frequency of the diocotron mode for arbitrary f has the form

$$\frac{\omega_1}{|\omega_{ce}|} = \frac{q}{4} \left(\frac{R_p^2}{R_w^2} - f \right) - \frac{k_z^2 R_p^2}{4}, \quad m = 1, \quad k_z R_p \ll 1, \quad q \ll q_{\max}. \quad (3.2)$$

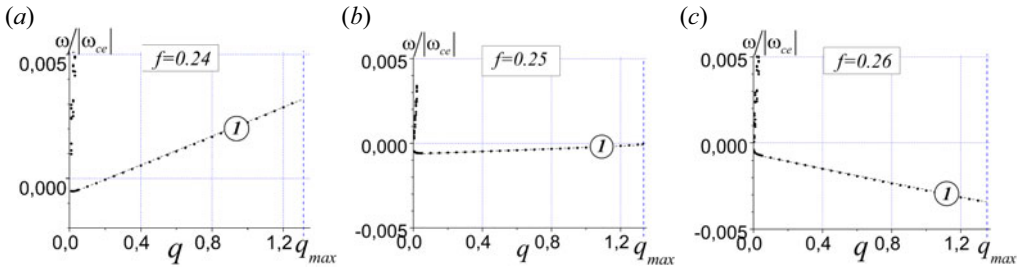


FIGURE 2. Behaviour of the long-wavelength ($k_z R_p \ll 1$) diocotron mode (‘1’) for values of the charge neutralization coefficient close to the value $f \approx R_p^2/R_w^2$ at which the transition from increasing to decreasing frequency occurs: (a) $f = 0.24$; (b) $f = 0.25$; (c) $f = 0.26$. The other calculation parameters are: $m = 1$; $k_z R_p = 0.05$; $R_p^2/R_w^2 = 0.25$.

Expression (3.2) agrees with the expression given by Levy *et al.* (1969) in § 7 for the case $k_z R_p = 0$. The correction to the frequency ω_1 due to $k_z R_p \neq 0$ is defined by Prasad & O’Neil (1983) for the case $f = 0$. As can be seen from (3.2) the correction is negative and does not depend on f and q .

As follows from (3.2), as well as is seen from figures 1 and 2, the sign of the frequency ω_1 and, in general, the behaviour of the diocotron mode are determined by three parameters: $k_z R_p$, R_p^2/R_w^2 , f . When $R_p^2/R_w^2 > f$ (figure 2a), the frequency ω_1 (3.2) increases with increasing q . When

$$q = q_0 = (k_z R_p)^2 / [(R_p/R_w)^2 - f] \quad (k_z R_p \ll 1, q_0 \ll q_{\max}), \tag{3.3}$$

frequency (3.2) reaches zero. It becomes positive at greater values of q .

When $R_p^2/R_w^2 < f$ (figure 2c), the frequency ω_1 decreases. It remains negative within the entire range of acceptable values of q .

When $R_p^2/R_w^2 \approx f$ (figure 2b), the frequency ω_1 remains close to zero within the entire range of acceptable values of q .

Numerical calculations according to the dispersion equation (2.1) for small values of $k_z R_p$ are presented in figure 2. They show that the behaviour of the diocotron mode is close to (3.2) within the entire range of acceptable values of q , except for very small values of q .

The behaviour of the diocotron mode (‘1’) at not a small value of $k_z R_p = 1$ (see figure 1) is not described by expression (3.2) and differs from its behaviour at small values of $k_z R_p$ (figure 2). However, the trend of shifting of the frequency of the diocotron mode towards negative frequencies with increasing f is observed both at small and at considerable values of $k_z R_p$.

3.6. Mode ‘2’ – cyclotron mode – is located near to the family of FUH modes and does not cross the low-frequency area. When $k_z R_p = 0$ the frequency of mode ‘2’ is determined by the expression (2.9.8) in Davidson (1974). When $k_z R_p \neq 0$ the frequency of mode ‘2’ is given by

$$\frac{\omega_2}{|\omega_{ce}|} \approx 1 - \frac{q}{4} \left[\left(\frac{R_p^2}{R_w^2} - f \right) - \frac{1}{2} \left(1 - \frac{R_p^2}{R_w^2} \right)^3 \frac{k_z^2 R_p^2}{4} \right], \quad m = 1, \quad k_z R_p \ll 1, \quad q \ll 1. \tag{3.4}$$

As is seen, the correction to the frequency ω_2 due to $(k_z R_p)^2$ is positive. Depending on the ratio between R_p^2/R_w^2 and f , the frequency ω_2 can be either less than or more than $|\omega_{ce}|$.

4. Conclusions about the behaviour of TG modes of non-neutral plasma

4.1. Trivelpiece–Gould modes form four families: two families of upper hybrid modes (SUH and FUH) and two families of lower hybrid modes (SLH and FLH).

There are also two modes that are located separately from these families: diocotron mode ('1') and cyclotron mode ('2'). The analytical expressions for their frequencies are given by expressions (3.2) and (3.4).

4.2. The upper hybrid modes of families SUH and FUH are extremely tightly spaced and very close to the upper hybrid frequency with a Doppler shift, $\omega \approx m\omega_{\text{rot}}^e \pm \omega_{\text{UH}}^{\text{NNP}}$. These modes (with an azimuthal number $m = 1$) do not cross the low-frequency area at any values of the parameters $k_z R_p$, R_w/R_p , f and q . Consequently, they cannot lead to resonance electron–ion instability.

4.3. The lower hybrid modes (SLH and FLH families) cross the low (ion)-frequency area. They can lead to resonance electron–ion instability.

4.4. The diocotron mode ('1') with a finite value of k_z crosses the low-frequency area, reaches the zero of the frequency at the value of q (3.3) and reverses the sign of frequency only if the waveguide is sufficiently fully filled with plasma: $(R_p/R_w)^2 > f$. In this case it can lead to resonance electron–ion instability.

Under the condition $(R_p/R_w)^2 \approx f$, the long-wavelength ($k_z R_p \ll 1$) diocotron mode is in the low-frequency area ($\omega \ll \omega_{\text{ce}}$) within the entire acceptable range of values of parameter q .

When $(R_p/R_w)^2 < f$, the diocotron mode does not cross zero frequency and cannot lead to resonance electron–ion instability (under the Cherenkov resonance condition $n = 0$ in (5.1)).

4.5. The cyclotron mode ('2') does not cross the low-frequency area. Its frequency ω_2 remains of the order of the cyclotron frequency of electrons $|\omega_{\text{ce}}|$ at any values of the parameter $q \leq q_{\text{max}}$ and of the charge neutralization coefficient f .

5. The electron–ion instability of non-neutral plasma, its expected characteristics and conditions of origin

So, the modes of the SLH family and the diocotron mode having an azimuthal number $m = 1$ can be of low frequency at definite values of the parameter q . At these values, these electron modes resonantly interact with ions. This will lead to the origin of resonance electron–ion instability. In this section we determine these resonance frequencies and corresponding values of q at which the frequency of the diocotron mode ('1') ω_1 equals the resonance ion frequencies. This will give an idea about the expected frequencies and growth rates of instability.

5.1. Resonance of an ion with a diocotron mode

The resonance condition between the transverse motion of an ion and a wave running along the azimuth in non-neutral plasma has the following form in the laboratory frame of reference (Davidson 1974):

$$\omega_{\text{res}} \approx m\omega_{\text{rot}}^i + n\Omega_i \quad (m = 0, +1, +2, \dots, n = 0, \pm 1, \pm 2, \dots). \quad (5.1)$$

Here

$$\omega_{\text{rot}}^i = (-\omega_{\text{ci}} + \Omega_i)/2 > 0 \quad (5.2)$$

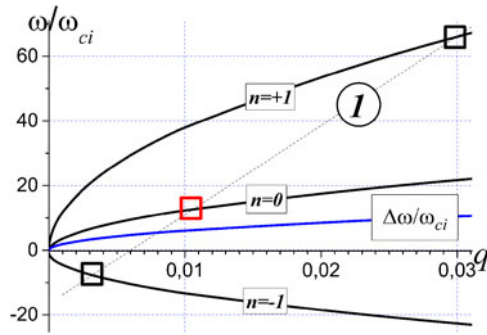


FIGURE 3. Resonance frequencies of ions (5.1) (denoted by black solid lines) for $m = +1$ and $n = +1, 0, -1$ and the frequency of the diocotron mode ω_1 (3.2) (denoted by a dotted line and the number ‘1’). The intersections of the frequencies are indicated by squares. The red square shows the Cherenkov resonance studied in the present article ($n = 0$). The dependence of $\Delta\omega$ (5.15) is also shown (blue solid line). All frequencies are normalized to ω_{ci} . Parameters of calculation: $m_i = 40$ a.u. (argon); $k_z R_p = 0.03$; $R_p/R_w = 0.5$; $f = 0.1$.

is the ‘slow’ ion rotation frequency, $\omega_{ci} = e_i B / (m_i c) > 0$ is the ion cyclotron frequency and

$$\Omega_i = \omega_{ci} [1 + (m_i/m_e)q(1-f)]^{1/2} = |\omega_{ce}| [(m_e/m_i)^2 + (m_e/m_i)q(1-f)]^{1/2} \quad (5.3)$$

is the ‘modified’ cyclotron frequency of ions.

As is shown in § 3.5, diocotron mode (‘1’) (3.2) reaches the area of low frequencies and the zero frequency only when $R_p^2/R_w^2 > f$ (see figure 2a). We consider this condition to be fulfilled. The dependencies on q of the diocotron mode (‘1’) (3.2) and of the resonance frequencies of ions (5.1) for $m = 1$ and multiplicities of resonances $n = -1, 0, +1$ are shown in figure 3.

In experiments (Vlasov *et al.* 1966; Nezlin 1982; Sakawa & Joshi 2000; Jaeger 2010; Annaratone *et al.* 2011; David 2017), unstable low-frequency oscillations rotating along the azimuth in the positive direction ($\omega/m > 0$) are observed. So, we study positive resonance frequencies. For $m = 1$ the lowest positive resonance ion frequency (5.1) is realized at $n = 0$. This is Cherenkov resonance between the diocotron mode and the ion rotation. The instability near this resonance was studied by Levy *et al.* (1969) in the hydrodynamic description of electrons and ions and $k_z = 0$. We determine the position of the resonance ($\omega_1 = \omega_{res}$) for $k_z \neq 0$. Substituting the expression for the frequency of the diocotron mode (3.2) into the left-hand side of (5.1) and putting $m = 1$ and $n = 0$ in the right-hand side, we obtain the following equation for q :

$$\frac{m_i}{2m_e} \left[q \left(\frac{R_p^2}{R_w^2} - f \right) - (k_z R_p)^2 \right] = -1 + \left[1 + \frac{m_i}{m_e} q(1-f) \right]^{1/2}. \quad (5.4)$$

By introducing a variable

$$y \equiv \frac{\Omega_i}{\omega_{ci}} = \left[1 + \frac{m_i}{m_e} q(1-f) \right]^{1/2} \geq 1, \quad (5.5)$$

we obtain a simpler equation for y :

$$\eta y^2 - 2y - \eta - k_z^2 R_p^2 (m_i/m_e) + 2 = 0. \quad (5.6)$$

In (5.6), the following notation is introduced:

$$\eta \equiv (R_p^2/R_w^2 - f)/(1 - f), \quad R_p^2/R_w^2 > f. \tag{5.7}$$

We are interested in the area $R_p^2/R_w^2 > f$ where η is positive. As follows from (5.7), the inequality $\eta < 1$ is always satisfied in this area.

From two roots of (5.6),

$$y = \eta^{-1}[+1 \pm \sqrt{(\eta - 1)^2 + \eta(k_z R_p)^2 m_i/m_e}], \tag{5.8}$$

only one root with the ‘+’ sign satisfies the inequality (5.5). We study only this root. It determines the resonance frequency of the ion (5.1) and the value of q at the point of intersection with the diocotron mode (3.2):

$$\omega_{\text{res}}/\omega_{\text{ci}} = (y - 1)/2, \quad q \equiv q_{\text{res}} = (m_e/m_i)(y^2 - 1)(1 - f)^{-1}. \tag{5.9a,b}$$

The resonance values (5.9) give an idea of the frequency and value of the parameter q near which the resonance electron–ion instability can arise.

Expressions (5.8) and (5.9) are simplified in limiting cases. When

$$[\eta/(\eta - 1)^2](k_z R_p)^2 \ll m_e/m_i, \tag{5.10}$$

solutions (5.9) take the form

$$\omega_{\text{res}}/\omega_{\text{ci}} \approx \frac{1 - R_p^2/R_w^2}{R_p^2/R_w^2 - f}, \quad q_{\text{res}} \approx 4 \frac{m_e}{m_i} \frac{1 - R_p^2/R_w^2}{(R_p^2/R_w^2 - f)^2}. \tag{5.11a,b}$$

The resonance frequency ω_{res} (5.11) is proportional to the ion cyclotron frequency ($\omega_{\text{res}} \propto \omega_{\text{ci}}$). The coefficient of proportionality is determined by the degree of filling of the waveguide with plasma (R_p^2/R_w^2) and by the degree of plasma charge neutralization (f). Expressions (5.11) do not depend on k_z . They are valid for sufficiently small values of $k_z R_p$ (5.10) and for the case $k_z R_p = 0$ studied by Levy *et al.* (1969).

The expression for q_{res} (5.11) gives numerical values that exactly correspond to the coordinates of the maxima of the growth rate obtained by Levy *et al.* (1969). These coordinates are presented by dotted lines in figure 2 of their article in variables f and $\lambda = 4(m_e/m_i)/[q(1 - f)]$. The analytical expression for resonance values of λ has the form

$$\lambda_{\text{res}} = 4 \frac{m_e}{m_i} \frac{1}{q_{\text{res}}(1 - f)} = \frac{(R_p^2/R_w^2 - f)^2}{[(1 - R_p^2/R_w^2)(1 - f)]}. \tag{5.12}$$

It is valid within the entire acceptable range of variations of f and R_p^2/R_w^2 . Expression (5.12) was written by Peurrung *et al.* (1993) for the case $f = 0$. The value of λ_{res} (5.12) does not depend on the mass of the ion (m_e/m_i).

The resonance frequency ω_{res} (5.11) is lower than the ion cyclotron frequency ($\omega_{\text{res}} < \omega_{\text{ci}}$) in the area

$$R_p^2/R_w^2 > (1 + f)/2. \tag{5.13}$$

This area is shown in figure 4. It takes the form of a triangle. On the lower boundary of the triangle, the equality $\omega_{\text{res}} = \omega_{\text{ci}}$ is fulfilled. On the upper boundary ($R_p^2/R_w^2 \rightarrow 1$), we have $\omega_{\text{res}} \rightarrow 0$.

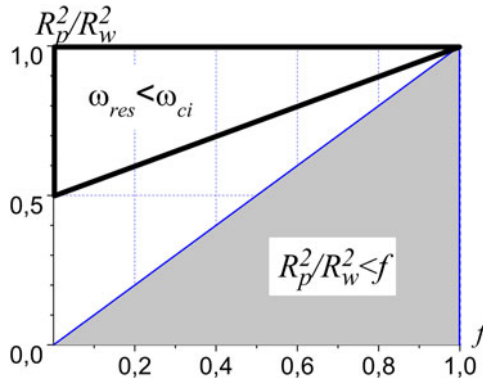


FIGURE 4. The area of low resonance frequencies ($\omega_{\text{res}} \leq \omega_{\text{ci}}$), with calculation using formula (5.11). The grey-shaded area in which $R_p^2/R_w^2 < f$ is not considered. The inequality (5.7) is not satisfied inside it.

If the inequality opposite to (5.10) is satisfied, the solution of the first equation (5.9) takes the following form:

$$\omega_{\text{res}}/\omega_{\text{ci}} \approx \frac{1}{2} \left\{ \frac{1 - R_p^2/R_w^2}{R_p^2/R_w^2 - f} + \left[\frac{(1 - f)}{(R_p^2/R_w^2 - f)} k_z^2 R_p^2 \frac{m_i}{m_e} \right]^{1/2} \right\}. \tag{5.14}$$

The value of q_{res} is determined by equation (5.9b). The second term in (5.14) is large compared with the first term. The resonance frequency (5.14) is always high compared with the ion cyclotron frequency ($\omega_{\text{res}} \gg \omega_{\text{ci}}$). Expression (5.14) gives a larger value of ω_{res} than expression (5.11). With a decrease in the parameter ($k_z R_p$), the frequency ω_{res} decreases to the level (5.11).

When $f \rightarrow R_p^2/R_w^2$ the value of q_{res} increases. Note that expressions (5.4)–(5.14), as well as (3.2), are valid when $k_z R_p \ll 1$, $q_{\text{res}} \ll q_{\text{max}}$.

5.2. Numerical estimations of resonance frequencies for typical values of experimental parameters

We obtain numerical values of the resonance frequencies from formulas (5.7)–(5.14) for experiments in which non-neutral plasma was produced as secondary plasma in an electron beam channel (Vlasov *et al.* 1966; Nezlin 1982; Sakawa & Joshi 2000; Jaeger 2010; Annaratone *et al.* 2011; David 2017).

We choose the following typical values of the experimental parameters. Geometrical parameters of the plasma cylinder: $R_p \sim 1$ cm; length, $L \sim 100$ cm. The degree of plasma charge neutralization $f = 0.1$, and the working gas is argon ($m_i = 40$ a.u., $m_e/m_i \approx 1.36 \times 10^{-5}$), which is often used in experiments. At first we estimate the minimum value of k_z for a plasma cylinder of finite length in the ‘usual’ way: $k_z \sim \pi/L$. We give estimations for different degrees of filling of the waveguide with plasma: $R_p/R_w = 0.5$; 0.75; 0.9. These values were used in calculations by Levy *et al.* (1969).

The inequality opposite to (5.10) is satisfied for chosen values of the parameters. In this case the resonance frequency ω_{res} and q_{res} are determined by formula (5.14). It gives the numerical values shown in table 1. Note that the values of ω_{res} and q_{res} for $R_p/R_w = 0.5$ are consistent with the position of the resonance in figure 3 (the red square).

The resonance frequencies in table 1 are high compared with the ion cyclotron frequency ω_{ci} . For lighter ions (for example, hydrogen, helium), a thinner or a longer plasma cylinder,

R_p/R_w	$\omega_{\text{res}}/\omega_{\text{ci}}$	q_{res}
0.5	13	1.2×10^{-2}
0.75	6.5	3×10^{-3}
0.9	4.95	1.3×10^{-3}

TABLE 1. The resonance frequency ω_{res} and q_{res} for different values of parameter R_p/R_w ($k_z R_p \simeq 0.03$, $f = 0.1$, $m_e/m_i \approx 1.36 \times 10^{-5}$ (argon)). Calculations are according to formula (5.14).

R_p/R_w	$\omega_{\text{res}}/\omega_{\text{ci}}$	q_{res}
0.5	5	1.8×10^{-3}
0.75	0.95	1.1×10^{-4}
0.9	0.27	2.1×10^{-5}

TABLE 2. The numerical values of resonance frequencies ω_{res} and q_{res} for different values of parameter R_p/R_w . The value of parameter $k_z R_p$ satisfies the inequality (5.10). Calculations are according to formula (5.11) ($f = 0.1$, $m_e/m_i \approx 1.36 \times 10^{-5}$ (argon)).

the left-hand side of inequality (5.10) can be of the same order as the right-hand side and even smaller. As a result, the resonance frequency will be determined by expression (5.11), which gives a smaller value of ω_{res} .

In such estimations, it is important to correctly take into account the finite value of k_z in experiments because of the sharp dependence of the diocotron frequency ω_1 (3.2) on k_z . The factor of finite plasma length, which is present in every experiment, greatly complicates the theoretical consideration of the stability problem. In this regard, we note the article by Prasad & O’Neil (1983), in which the eigenfrequencies and eigenmodes of a long ($R_p/L \ll 1$) plasma cylinder of finite length, located in an infinite metal cylindrical waveguide, are determined. They showed that in such a plasma model the diocotron mode has a longitudinal wavelength that is much longer than the plasma length: $|k_z| \sim [(1/|\varepsilon_3|)(L/R_p)]^{1/2}(1/L) \ll (1/L)$. Evaluating $|\varepsilon_3| \sim 8/[q(1-f)^2]$ according to (2.8), we find the following value of the parameter $k_z^2 R_p^2$: $k_z^2 R_p^2 \sim (1-f)^2(q/8)(R_p/L)$. When $q \ll 8(L/R_p)(m_e/m_i)$ the value of $k_z^2 R_p^2$ satisfies inequality (5.10), and the resonance values ω_{res} and q_{res} are determined by expressions (5.11). The numerical values for this case are shown in table 2. As is seen from table 2 and figure 4, in the long-wavelength limit, when inequality (5.10) is satisfied, the resonance frequency ω_{res} can be both low and high compared with the ion cyclotron frequency ω_{ci} . When the waveguide is sufficiently fully filled with plasma (see formula (5.13)), the resonance frequency is small compared with the cyclotron frequency or of the same order of magnitude.

5.3. Expected frequencies of electron–ion instability

What frequency ω of the discussed non-neutral plasma instability due to the relative motion of electrons and ions along the azimuth can be expected? Generally speaking, its frequency is not equal to the resonance frequency (5.1).

This instability was studied by Levy *et al.* (1969) (see also Davidson 1974). They described thresholds and maximum growth rates of instability in detail. However, the

expression for the real part of the unstable frequency has not been calculated and written out explicitly. It seems that this is one of the reasons why this powerful instability, the conditions of the origin of which always exist in non-neutral plasma, was not used to explain the nature of low-frequency oscillations in linear devices, in which non-neutral plasma was produced in the electron beam channel (Vlasov *et al.* 1966; Nezlin 1982; Pierre *et al.* 1987; Sakawa & Joshi 2000; Jaeger 2010; Annaratone *et al.* 2011; David 2017).

There is also another reason. In the article by Levy *et al.* (1969) it is stated that, for $f \ll 1$, the instability occurs only near the resonance of the diocotron mode with the ion rotation. The term ‘resonance’ was even included in the title of the paper. However, in experiments, the instability is observed in a wide range of field variations, i.e. outside the resonance too. This difference, noted by Peurrung *et al.* (1993), makes the instability of Levy *et al.* (1969) unlike the instability observed in experiments. This shortcoming of the theory was overcome by Fajans (1993) in the framework of the nonlinear consideration.

This shortcoming can also be overcome within the framework of the linear theory of stability, taking into account kinetics of ions in the plasma model considered by Levy *et al.* (1969).

The hydrodynamic description of ions used by Levy *et al.* (1969) is not applicable when ions are unmagnetized ($q \geq m_e/m_i$). Ions are produced in experiments by electron impact of atoms (molecules) of the working (residual) gas. In crossed fields they oscillate along the radius with an amplitude comparable to the radius of the plasma cylinder itself. A detailed analysis of ion kinetics in crossed fields was also carried out by Levy *et al.* (1969). A solution of the kinetic equation for ions was even obtained in that paper. But these results were not used in the study of instability. For such ions, a kinetic description is absolutely necessary.

The equilibrium distribution function of ions, which adequately takes into account the peculiarities of their production in crossed fields, was determined by Dem’yanov *et al.* (1988). It turned out to be anisotropic and non-Maxwellian in transverse energies and, therefore, very unstable. Due to anisotropy of ions such plasma is unstable even without the resonance with the electron mode (Mikhailovskii 1974; Yeliseyev 2006). The stability of non-neutral plasma with such an ion distribution function was investigated by Yeliseyev (2010) for a waveguide completely filled with plasma, $m = 1$, $k_z \neq 0$ and $f \ll 1$. It is shown that near every harmonic of the ion resonance frequency (5.1) there exist not one, but two ion modes. The frequency of one of them is lower than the ion resonance frequency, the frequency of the other is higher. Both modes exist within the entire acceptable range of variation of the parameter q . Their frequencies repeat the dependence on q of ion resonance frequency (5.1). They are called ‘modified’ ion cyclotron modes. In the resonance area the electron mode is unstable with a fast growth rate. In a wide region outside the resonance, where $q < q_{\text{res}}$, the lower modified ion cyclotron mode is unstable, but with a slower growth rate ($\text{Im } \omega \equiv \gamma \sim \omega_{\text{pi}}$). The real part of the frequency ($\text{Re } \omega$) of the unstable mode in the area $q < q_{\text{res}}$ remains lower than the resonance frequency (5.1) by the value $\Delta\omega$ (Yeliseyev 2010):

$$\begin{aligned} \Delta\omega &\equiv |\text{Re } \omega - \omega_{\text{rot}}^i| \sim \gamma \sim \omega_{\text{pi}} = \omega_{\text{ce}}[q(f/2)(m_e/m_i)]^{1/2} \\ &= \omega_{\text{ci}}[q(f/2)(m_i/m_e)]^{1/2} \simeq \Omega_i[f/(1-f)]^{1/2}. \end{aligned} \quad (5.15)$$

The dependence of $\Delta\omega$ (5.15) on q is shown in figure 3.

The resonance frequency (5.1) does not depend on the degree of filling of the waveguide (R_p^2/R_w^2). So, it can be supposed that the value of $\Delta\omega$ (5.15) has the same order of magnitude when the waveguide is partially filled with plasma ($R_p^2/R_w^2 < 1$). Because of the decrease in the value of $\Delta\omega$ (5.15), the real part of the frequency $\text{Re } \omega$ can become

comparable to the cyclotron frequency ω_{ci} . The real part of the frequency $\text{Re}\omega$ will behave depending on q in a manner similar to how $\Delta\omega$ behaves in [figure 3](#).

In addition, the resonance frequency ω_{res} (5.1), which in the considered case of Cherenkov resonance equals ω_{rot}^i (5.2), itself decreases with a decrease in q . With it the frequency of unstable oscillations $\text{Re}\omega$ decreases (see [figure 3](#)). Taking into account these two circumstances, the triangular area in [figure 4](#), where $\omega_{\text{res}}/\omega_{ci} \leq 1$, must be larger than is shown in the figure.

The equalities (5.15) contain also an estimation of the growth rate of instability $\text{Im}\omega = \gamma$. This is consistent with the frequency correction $\Delta\omega$. So the dependence of the growth rate γ on q looks like the dependence of $\Delta\omega$ in [figure 3](#). From (5.15) it follows that the growth rate exceeds the ion cyclotron frequency ($\gamma > \omega_{ci}$) in the area where $qf > 2m_e/m_i$. This inequality is satisfied in a wide range of acceptable parameter values.

Summarizing the above, we conclude that the diocotron mode interacting with ions having an anisotropic distribution function can lead to electron–ion instability at frequencies $\text{Re}\omega$, which can be comparable to the ion cyclotron frequency ω_{ci} , and have fast growth rates ($\text{Im}\omega = \gamma > \omega_{ci}$) within a wide range of variations of parameter q , as is observed in experiments.

There is also an area of parameters in which the instability frequencies are large compared with the cyclotron frequency. Note that in different experiments with non-neutral plasma, produced in an electron beam channel, unstable oscillations are observed both at low frequencies $\omega < \omega_{ci}$ (Jaeger 2010; Annaratone *et al.* 2011; David 2017) and at much higher frequencies (5–10) ω_{ci} (Sakawa & Joshi 2000).

5.4. About the instability of SLH modes

The family of SLH modes also passes through zero frequency and through the low-frequency area and can also be the cause of electron–ion instability. In the long-wavelength limit ($k_z R_p \ll 1$), SLH modes pass zero frequency at small values of q , while the diocotron mode crosses the value of zero of frequency at larger values of q (see [figure 1a](#)). Correspondingly, the growth rate of the instability associated with the diocotron mode is faster than the growth rates associated with the SLH modes. Note that the instability associated with the diocotron mode must develop at higher frequency than the instabilities associated with the SLH modes.

In the long-wavelength limit ($k_z R_p \ll 1$), the SLH modes are closely spaced around the value of $\omega = \omega_{\text{rot}}^e$. Different radial modes of this family can be excited with a small variation of the parameter q . However, in experiments, within a wide range of variation of fields, only the lowest radial mode is excited. This circumstance does not allow one to associate the observed low-frequency oscillations with SLH modes. The diocotron mode interacting with ions seems to be more preferable for explaining the nature of low-frequency oscillations observed in experiments with non-neutral plasma in linear devices (Vlasov *et al.* 1966; Nezlin 1982; Sakawa & Joshi 2000; Jaeger 2010; Annaratone *et al.* 2011; David 2017) and other similar experiments.

6. Conclusions

We discussed the electron–ion instability that arises in non-neutral plasma due to the interaction of the diocotron mode with ions. It occurs due to the relative motion of electrons and ions along the azimuth, due to the anisotropy of the ion distribution function and finite value $k_z \neq 0$. This instability has the same characteristics as the low-frequency oscillations observed in experiments in linear devices, where non-neutral plasma is created as a secondary plasma in the electron beam channel (Vlasov *et al.* 1966; Nezlin 1982;

Pierre *et al.* 1987; Sakawa & Joshi 2000; Jaeger 2010; Annaratone *et al.* 2011; David 2017):

- (1) The discussed instability can be of low frequency ($\omega \sim \omega_{ci}$) in the long-wavelength limit $k_z R_p \ll 1$, like the oscillations observed in experiments.
- (2) The instability occurs within a wide range of variations of external fields and plasma parameters both near the resonance of the diocotron mode with ions and outside this resonance area ($q < q_{res}$).
- (3) The unstable mode has the structure of the lowest radial mode (see Prasad & O’Neil 1983). Oscillations with only such a radial dependence are observed in experiments.
- (4) The growth rate of the discussed instability can be fast compared with the cyclotron frequency ($\gamma > \omega_{ci}$) within a wide area of parameter variations ($qf > 2m_e/m_i$). A fast increase of the amplitude of low-frequency oscillations (during a time less than the period of oscillations) is observed in experiments (Jaeger 2010; David 2017).

In non-neutral plasma, there is always a relative motion of electrons and ions along the azimuth and there is always an anisotropy of produced ions. Thus, there are always conditions for the origin of the instability caused by these reasons. This instability can be the cause of the observed low-frequency oscillations of non-neutral plasma in linear devices.

Acknowledgements

Editor Francesco Califano thanks the referees for their advice in evaluating this article.

Funding

This work was partially supported by a grant of the National Academy of Sciences of Ukraine (X-3-19-10-2019).

Declaration of interests

The author reports no conflict of interest.

Appendix A. Areas of existence of bulk and surface modes

We determine the areas where the TG modes in the plasma are bulk or surface modes. This is determined by the sign of T^2 (2.2). Modes located in the area $T^2 > 0$ are bulk modes. The dependence of their potential on the radius has the form $J_m(Tk_z r)$ in plasma. Modes located in the area $T^2 < 0$ are surface modes. The dependence of their potential has the form $I_m(|T|k_z r)$. The boundaries between the areas are located on the lines where the function T^2 reverses sign. This is determined by the reversal of the sign of the tensor components ε_1 and ε_3 .

In variables (ω^2/ω_{ce}^2 , q) the shape of the boundaries has an extremely simple form (figure 5). The areas where $T^2 > 0$ and modes are bulk are indicated by arrows. In non-neutral plasma ($f < 1$) the areas are two triangles. In neutral plasma ($f = 1$) the areas are two bands. In both cases, the two areas touch at the point with coordinates

$$q = q_t \equiv 2/(3 - 2f), \quad \omega^2/\omega_{ce}^2 = q_t/2 = 1/(3 - 2f). \quad (\text{A1a,b})$$

At the touchpoint the equalities $\omega^2 = \omega_{pe}^2 = \Omega_e^2$ are satisfied (Davidson 1974).

In other areas, we have $T^2 < 0$. The modes located in these areas are surface modes.

Function T^2 (2.2) does not depend on the degree of filling of the waveguide (R_p^2/R_w^2) and on the longitudinal wavelength $k_z R_p$. The position of the borders does not depend on them

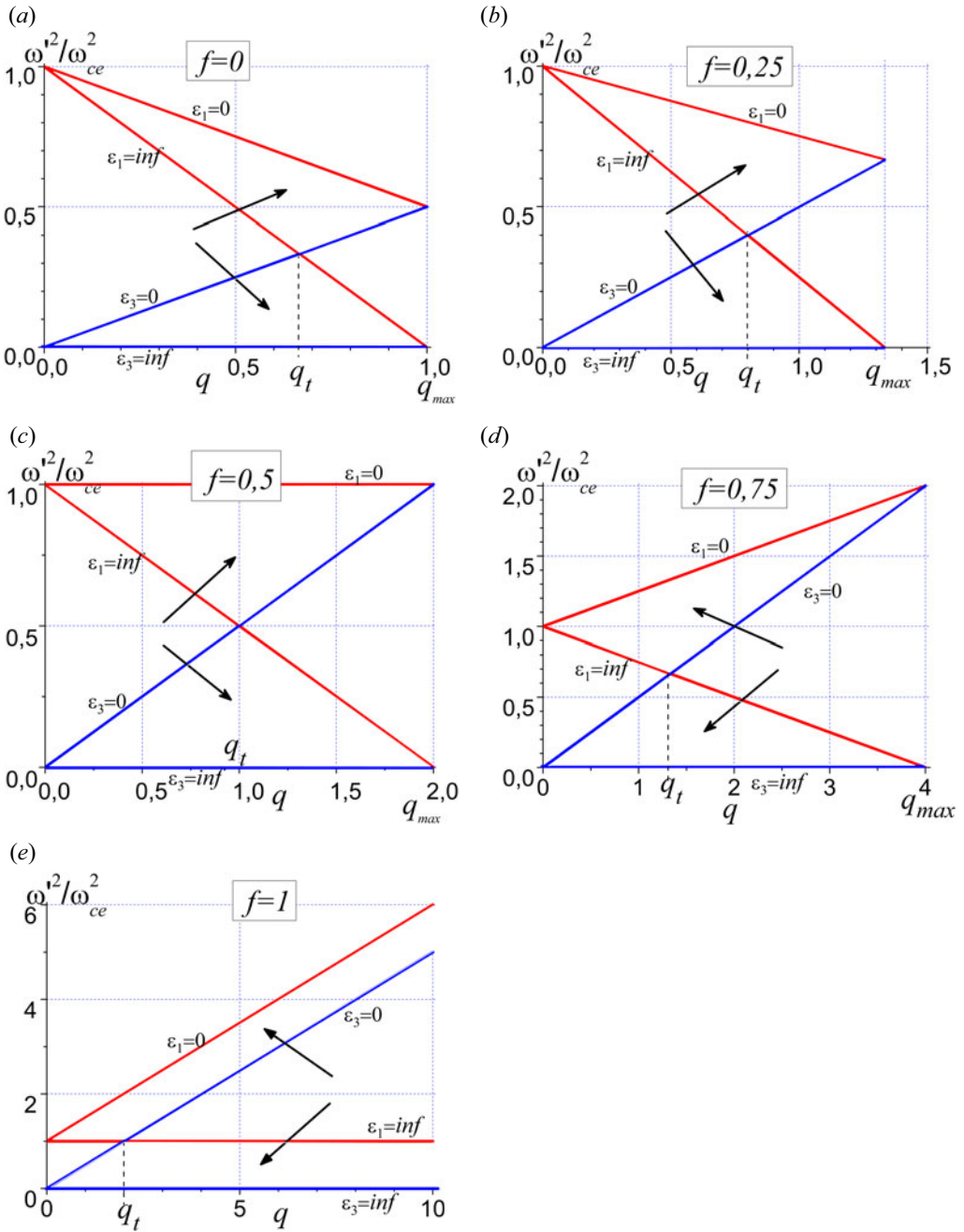


FIGURE 5. The areas of existence of bulk modes (indicated by arrows) and surface modes on the plane of variables $(\omega^2/\omega_{ce}^2, q)$ for different values of the charge neutralization coefficient f : (a) $f = 0$; (b) $f = 0.25$; (c) $f = 0.5$; (d) $f = 0.75$; (e) $f = 1$. The red and blue solid lines show the zeros and poles ($\epsilon_{1,3} = \text{inf}$) of tensor components ϵ_1 and ϵ_3 (2.8). Parameters q_{max} and q_t are defined by (1.2) and (A 1).

either. The simplicity of figure 5 indicates the successful choice of variables with which the figures are built.

On the plane of variables $(\omega/\omega_{ce}, q)$ (see figure 1), the areas of bulk modes ($T^2 > 0$) are transformed into four areas. They have the form of curvilinear triangles. In figure 1 they are indicated by arrows.

From figure 1 it can be seen that families of FLH, SLH, FUH and SUH modes are located within the bulk areas. The areas of the bulk modes in figure 5 are consistent with the areas where the inequality (3.1) is satisfied.

It can be seen from figure 1 that diocotron ('1') and cyclotron ('2') modes are bulk modes at sufficiently small q . They are surface modes at larger values of q .

Appendix B. Trivelpiece–Gould modes of waveguide partially filled with neutral plasma

B.1. The solutions of the dispersion equation (2.1) for neutral plasma ($f = 1$) are shown in figure 1(e). Solutions exist for all values of q from the interval $0 < q < \infty$. In figure 1(e) they are represented within the interval $0 \leq q \leq 10$.

The structure of the solutions for neutral plasma is, in general, the same as that for non-neutral plasma. The solutions form four families of modes marked FLH, SLH, FUH and SUH. But the meanings of the terms 'fast' (F) and 'slow' (S) modes in a neutral plasma are lost, because plasma does not move and there is no Doppler shift ($\omega' = \omega$). These four families are located in the frequency intervals (3.1). In expressions (3.1) it is necessary to replace $\omega' \rightarrow \omega$, $\Omega_e \rightarrow \omega_{ce}$.

When plasma partially fills the waveguide, the mode frequencies of all four families are slightly shifted upward, towards positive frequencies. The frequencies of the modes of FUH and SUH families shift negligibly. The asymmetry in the location of modes is caused by the last term on the right-hand side of the dispersion equation (2.1) and is a demonstration of the plasma magnetoactivity.

Along with the four families of modes, there are two more separate modes, indicated in figure 1(e) as '1' and '2'. In non-neutral plasma mode '1' is called a diocotron mode. In neutral plasma, the frequency of this mode (azimuthal phase velocity ω_1/m) is always negative. This also follows from expression (3.2).

The frequency of mode '2' is always positive and always exceeds the cyclotron frequency: $|\omega_{ce}| < \omega_2 < \omega_{UH}$ ($\omega_{UH} = \sqrt{\omega_{pe}^2 + \omega_{ce}^2}$ is a hybrid frequency of the neutral plasma). This follows from expression (3.4).

At sufficiently small q , modes '1' and '2' are located in the frequency range (3.1) and are bulk modes. As q grows, they go beyond the frequency areas (3.1) and become surface modes.

As the degree of filling of the waveguide with plasma increases ($(R_p/R_w)^2 \rightarrow 1$), mode '1' approaches the family of SLH modes. Mode '2' moves away from the FUH family of modes and approaches the frequency $|\omega_{ce}|$. These peculiarities of the behaviour of modes '1' and '2' are also seen from expressions (3.2) and (3.4).

When $q \neq 0$, no TG modes pass through the low-frequency region, do not cross zero frequency and, therefore, cannot lead to the resonance electron–ion instability.

B.2. The frequencies of potential modes of a waveguide partially filled with neutral plasma were determined and studied by Trivelpiece & Gould (1959). The dependences of frequencies of TG modes on the longitudinal wave vector k_z are represented in figure 8 of their paper. In figure 6 the solutions of the dispersion equation (2.1) are shown for the same values of the parameters, with the difference that in present paper the azimuthal number m is considered positive ($m = +1 > 0$), and the mode frequencies ω can be positive and

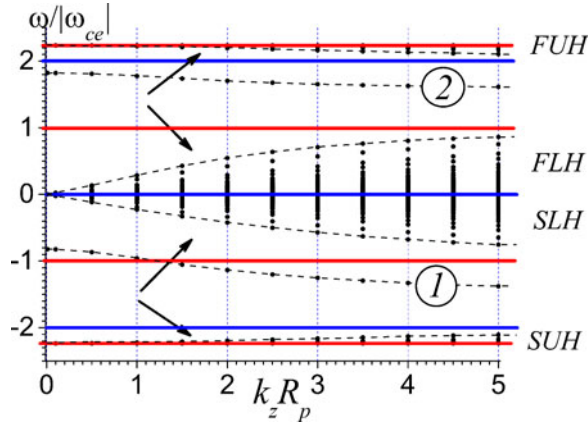


FIGURE 6. Trivelpiece–Gould modes of a waveguide partially filled with neutral plasma ($f = 1$). The calculation parameters are the same as in figure 8 of Trivelpiece & Gould (1959): $m = 1$; $f = 1.0$; $R_w/R_p = 2.0$; $q = 8.0$. The lowest radial modes of the FLH, SLH, FUH and SUH families and modes ‘1’ and ‘2’ are indicated by dashed lines. The arrows indicate the bands where the modes are bulk modes. The borders of the bands are delimited by solid blue and red lines.

negative. In the paper by Trivelpiece & Gould (1959), the frequencies ω were considered positive, and the azimuthal number m was considered positive and negative ($m = \pm 1$).

Comparison of figure 8 of Trivelpiece & Gould (1959) and figure 6 here shows that the modes located at the bottom of figure 8 marked ‘+1’ and ‘−1’ correspond in figure 6 to the lowest radial modes of the FLH and SLH families, respectively (indicated by dotted lines). The modes located at the top of figure 8 of Trivelpiece & Gould (1959), marked ‘ $n = +1$ ’ and ‘−1’, correspond in figure 6 here to the modes marked by the numbers ‘2’ and ‘1’, respectively. The upper hybrid modes of the FUH and SUH families are not displayed in figure 8 of Trivelpiece & Gould (1959). They are located above the frequency range shown in the figure.

The behaviour of the modes in both figures looks identical, but in figure 6, the frequencies ω are normalized to $|\omega_{ce}|$, while in figure 8 of Trivelpiece & Gould (1959), the normalization to ω_p is erroneously indicated. The normalization to $|\omega_{ce}|$ is correct.

Note that mode ‘2’ is a surface mode within the entire range of values of parameter $k_z R_p$ presented in figure 6. Mode ‘1’ is a bulk mode at rather small values of $k_z R_p$, approximately at $k_z R_p < 1.2$. At larger values of $k_z R_p$, mode ‘1’ becomes a surface mode.

REFERENCES

- ANNARATONE, B.M., ESCARGUEL, A., LEFEVRE, T., REBONT, C., CLAIRE, N. & DOVEIL, F. 2011 Rotation of magnetized plasma. *Phys. Plasmas* **18**, 032108.
- BETTEGA, G., CAVALIERE, F., CAVENAGO, M., ILLIBERI, A., POZZOLI, R. & ROMÉ, M. 2005 Experimental investigation of the ion resonance instability in a trapped electron plasma. *Plasma Phys. Control. Fusion* **47**, 1697.
- DAVID, P. 2017 Tomography in a linear magnetized plasma. PhD thesis, Aix-Marseille Université.
- DAVIDSON, R.C. 1974 *Theory of Nonneutral Plasmas*, 215 p. Benjamin.
- DEM’YANOV, V.G., YELISEYEV, Y.N., KIROCHKIN, Y.A., LUCHANINOV, A.A., PANCHENKO, V.I. & STEPANOV, K.N. 1988 Equilibrium and nonlocal ion cyclotron instability of plasma in crossed longitudinal magnetic and strong radial electric fields. *Sov. J. Plasma Phys.* **14**, 494.

- DUBIN, D.H.E. 2016 Penning traps and plasma modes. In *Trapped Charged Particles: A Graduate Textbook with Problems and Solutions* (ed. M. Knoop, N. Madsen & R.C. Thompson). World Scientific.
- FAJANS, J. 1993 Transient ion resonance instability. *Phys. Fluids B* **5**, 3127–3135.
- JAEGER, S. 2010 Etude theorique et experimentale des instabilites basses frequences dans un plasma en champs magnetique et electrique croises. PhD thesis, Aix-Marseille Universite.
- KABANTSEV, A.A. & DRISCOLL, C.F. 2003 Diocotron instabilities in an electron column induced by a small fraction of transient positive ions. *AIP Conf. Proc.* **692**, 61–68.
- LEVY, R.H., DAUGHERTY, J.D. & BUNEMAN, O. 1969 Ion resonance instability in grossly nonneutral plasma. *Phys. Fluids* **12**, 2616–2629.
- MIKHAILOVSKII, A.B. 1974 *Theory of Plasma Instabilities, V. 1: Instabilities of a Homogeneous Plasma*. Consultants Bureau.
- NEZLIN, M.V. 1982 *Beam Dynamics in Plasma*. Energoizdat (in Russian).
- PEURRUNG, J., NOTTE, J. & FAJANS, J. 1993 Observation of the ion resonance instability. *Phys. Rev. Lett.* **70**, 295–298.
- PIERRE, T., LECLERT, G. & BRAUN, F. 1987 Magnetized double-plasma device for wave studies. *Rev. Sci. Instrum.* **58**, 6–11.
- PRASAD, S.A. & O'NEIL, T.M. 1983 Waves in a cold pure electron plasma of finite length. *Phys. Fluids* **26**, 665–672.
- SAKAWA, Y. & JOSHI, C. 2000 Growth and nonlinear evolution of the modified Simon-Hoh instability in an electron beam-produced plasma. *Phys. Plasmas* **7**, 1774–1780.
- TRIVELPIECE, A.W. & GOULD, R.W. 1959 Space charge waves in cylindrical plasma columns. *J. Appl. Phys.* **30**, 1784–1793.
- VLASOV, M.A., DOBROKHOTOV, E.I. & ZHARINOV, A.V. 1966 Instability of a hot-cathode discharge in a magnetic field at low pressures. *Nucl. Fusion* **6**, 24–34.
- YELISEYEV, Y.N. 2006 Nonlocal theory of the spectra of modified ion cyclotron oscillations in a non-neutral plasma produced by gas ionization. *Plasma Phys. Rep.* **32**, 927–936.
- YELISEYEV, Y.N. 2010 Oscillation spectrum of an electron gas with a small density fraction of ions. *Plasma Phys. Rep.* **36**, 563–582.